

Direct Adversarial Training: A New Approach for Stabilizing The Training Process of GANs

Ziqiang Li, Pengfei Xia, Rentuo Tao, Hongjing Niu and Bin Li*

CAS Key Laboratory of Technology in Geo-spatial Information Processing and Application Systems
University of Science and Technology of China, Anhui, China

ARTICLE INFO

Keywords:

Adversarial training, Generative adversarial networks, Lipschitz.

ABSTRACT

Generative Adversarial Networks (GANs) are the most popular models for image generation by optimizing discriminator and generator jointly and gradually. However, instability in training process is still one of the open problems for all GAN-based algorithms. In order to stabilize training, some regularization and normalization techniques have been proposed to make discriminator meet the Lipschitz continuity constraint. In this paper, a new approach inspired by works on adversarial attack is proposed to stabilize the training process of GANs. It is found that sometimes the images generated by the generator play a role just like adversarial examples for discriminator during the training process, which might be a part of the reason of the unstable training. With this discovery, we propose to introduce a adversarial training method into the training process of GANs to improve its stabilization. We prove that this DAT can limit the Lipschitz constant of the discriminator **adaptively**. The advanced performance of the proposed method is verified on multiple baseline and SOTA networks, such as DCGAN, WGAN, Spectral Normalization GAN, Self-supervised GAN and Information Maximum GAN.

1. Introduction

Recently, Generative Adversarial Networks (GANs) [7] have been used in many generative tasks, such as image inpainting [43, 40], attribute editing [35, 32], and adversarial examples [39, 33]. GANs are two-player zero-sum games, in which a discriminator measures the distance between generated and real distributions, while a generator tries to fool the discriminator by minimizing the distance between real and generated distributions. Specifically, vanilla GAN [7] trains a critic to approximate the JS divergence, f -GAN [25] and WGAN [1] train a critic to approximate the f divergence and Wasserstein divergence, respectively. According to the optimal transport theory [3], Wasserstein distance is the transportation cost of the optimal transportation map. The solution for Wasserstein divergence can be got by Kantorovich duality [12], which is existing and unique. In order to solve the Kantorovich duality problem of the Wasserstein distance, the discriminator should meet the 1-Lipschitz constraint. This is the first time that Lipschitz continuous has been used for training of GANs. Except for 1-Lipschitz constraint in WGANs, Lipschitz constraint is important for generalizability and distributional consistency for GANs [28]. Qi [28] proved that, for the discriminator with Lipschitz continuous, the generated distributions converge to the real distributions in WGANs.

Vulnerable to adversarial examples [34] is a problem that often occurs in neural networks. Small perturbations added on input samples can incur error predictions like misclassi-

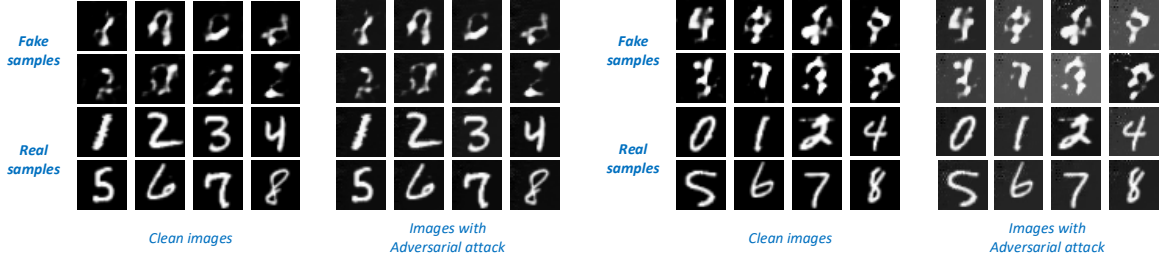
fication even for the most advanced deep neural networks. Empirically, the most effective strategy to defense against adversarial attacks is adversarial training [8], which uses adversarial examples to train the classifier improving the robustness of the models. Inspired by adversarial examples in deep neural networks, we argue that the instability of GANs' training has close relation with adversarial examples generated by the generator which can fool the discriminator. Based on the above assumptions, we first do a confirmatory experiment which attack the discriminator of DCGAN [29]. The result is shown in Fig.1. The success of the attack is defined as:

$$\begin{aligned} |D(\hat{x}_f) - D(x_r)| &\leq 0.02, \\ |D(\hat{x}_r) - D(x_f)| &\leq 0.02, \end{aligned} \quad (1)$$

where D represents the discriminator, x_f and x_r denote fake images generated by non-convergent generator and real images sampled from train datasets, respectively. \hat{x}_f and \hat{x}_r are adversarial examples of generated images and real images, respectively. From Fig.1 (a), we can see that average iterations for successfully attacking a discriminator without adversarial training are 3.2 and 3.88, which indicates that vanilla GAN models can be easily attacked. Also, we can not distinguish between clean images and adversarial examples, intuitively. Since the model is assumed to have infinite capacity [7], without any prior, the generator has a high probability to generate adversarial examples that can mislead the discriminator, which makes the training of GANs unstable. Moreover, we also give the proof of the existence of adversarial examples in the following chapters. To avoid the above mentioned unstable threats, this paper proposes a method called direct adversarial training for GANs' training, which reduces the Wasserstein distance between real and generated distributions, and improves the quality of the generated images. The main contributions can be summarized as follows:

*corresponding author

✉ iceli@mail.ustc.edu.cn (Z. Li); xpengfei@mail.ustc.edu.cn (P. Xia); trtmelon@mail.ustc.edu.cn (R. Tao); sasori@mail.ustc.edu.cn (H. Niu); binli@ustc.edu.cn (B. Li)
✉ <http://staff.ustc.edu.cn/~binli/> (B. Li)
ORCID(s):



(a) adversarial attack without the adversarial training

$$(\bar{K}_{fake} = 3.2, \bar{K}_{real} = 3.88)$$

(b) adversarial attack with the adversarial training

$$(\bar{K}_{fake} = 37.36, \bar{K}_{real} = 7.44)$$

Figure 1: Adversarial attack with the discriminator. (a) and (b) are the adversarial samples when DCGAN has no adversarial training and adversarial training on Mnist, respectively. Top two lines are the fake samples which are generated by generator without convergence. Bottom two lines are real samples from Mnist dataset. \bar{K}_{fake} and \bar{K}_{real} are the average number of iterations when fake images and real images are successfully attacked, respectively

- We prove that the generator may generate adversarial examples of the discriminator during the training of GANs and analyze the adversarial attack of the discriminator for the first time.
- We propose Direct Adversarial Training (DAT) for stabilizing the training process of GANs and prove that the DAT can **adaptively** adjust Lipschitz continuous of the discriminator, which is different from the gradient penalty proposed by previous work.
- Despite the simplifications, our method surprisingly improves the quality of the generated images on many basic and SOTA models.

2. Background and Related Work

2.1. Generative Adversarial Networks

GANs are two-player zero-sum games, where the generator $G(z)$ is a distribution mapping function that transforms samples of a low-dimensional latent distribution z into samples from the target images distribution p_g . The generator is trained with another network $D(x)$, which evaluates the distance between generated distribution p_g and real distribution p_r . The generator and discriminator minimize and maximize the distribution distance respectively. This minimax game can be expressed as:

$$\begin{aligned} \min_{\phi} \max_{\theta} f(\phi, \theta) = & \mathbb{E}_{x \sim p_r} [g_1(D_{\theta}(x))] \\ & + \mathbb{E}_{z \sim p_z} [g_2(D_{\theta}(G_{\phi}(z)))] \end{aligned} \quad (2)$$

where ϕ and θ are parameters of the generator G and discriminator D , respectively. Specifically, vanilla GAN [7] can be described by $g_1(t) = g_2(-t) = -\log(1 + e^{-t})$, f-GAN [25] and WGAN [1] can be written as $g_1(t) = -e^{-t}$, $g_2(t) = 1 - t$ and $g_1(t) = g_2(-t) = t$, respectively.

2.2. Lipschitz Constant and WGAN

Lipschitz constant of the function $f : X \rightarrow Y$ is defined by:

$$\|f\|_L = \sup_{x \in X, x \neq y} \frac{\|f(x) - f(y)\|}{\|x - y\|}. \quad (3)$$

Intuitively, the function f is called K-Lipschitz continuous, if there exists a constant $K \geq 0$ for which $\|f(x) - f(y)\| \leq K\|x - y\|$ for any $x, y \in X$. Theoretically, Lipschitz constant of the neural network can be approximated by spectral norm of the weight matrix [17]:

$$\|W\|_2 = \max_{x \neq 0} \frac{\|Wx\|}{\|x\|}. \quad (4)$$

The Lipschitz constant can be used to express the Lipschitz continuous of a neural network. The low Lipschitz constant means that the neural network is less sensitive to input perturbation and the bounded Lipschitz constant indicates that the network has better generalization [41, 26, 6].

For GANs, a lot of works are proposed to limit the Lipschitz constant of the discriminator. The main methods are spectral normalization [23] and WGAN [1]. Spectral normalization normalizes the spectral norm of the discriminator, which limits its Lipschitz constant to 1. And the Lipschitz constant in WGAN is derived from Kantorovich duality [12], the Wasserstein distance corresponding to the optimal transportation can be represented as:

$$W(P_1, P_2) = \sup_{\|f\|_L=1} \mathbb{E}_{x \sim p_r} f(x) - \mathbb{E}_{x \sim p_g} f(x), \quad (5)$$

where $f : X \rightarrow \mathbb{R}$ is called the Kantorovich potential, which can be used as discriminator. In order to make the discriminator satisfy the lipschitz continuous, WGAN [1] uses the weight clipping which restricts the maximum value of each weight; WGAN-GP [9] uses the gradient penalty with the interpolation of real samples and generated samples: $\hat{x} = tx + (1 - t)y$ for $t \sim U[0, 1]$ and $x \sim P_r, y \sim P_g$

being a real and generated samples; WGAN-ALP [36] inspired by Virtual Adversarial Training (VAT) [24] restricts the 1-Lipschitz continuous at $\hat{x} = \{x, y\}$ with the direction of adversarial perturbation. Different from the above methods which restrict the 1-Lipschitz continuous [9, 36, 13, 49], WGAN-LP [27] restricts the k -Lipschitz continuous ($k \leq 1$), which is derived from the optimal transport with regularization. Also, Qi. [28] is motivated to have lower sample complexity by directly minimizing the Lipschitz constant rather than constraining it to 1, which can be described as 0-GP [48, 22, 37]. In summary [17], there are many methods for restricting the Lipschitz constant, some restrict the constant to 1, some restrict it to k ($k \leq 1$), and some minimize the Lipschitz constant.

2.3. Adversarial Examples and Adversarial Training

Adversarial examples are a common problem in neural networks. Given a pre-trained model h , an adversarial example x' is defined by $x' = x + \delta$ with $h(x') \neq h(x)$ for untargeted attack or $h(x') = t$ for targeted attack, where x is a clean image and δ is an imperceptible tiny perturbation. There are many methods to generate adversarial examples, such as Fast Gradient Sign Method (FGSM) [8], Basic Iterative Methods (BIM) [15], and Projected Gradient Descent (PGD) [20]. FGSM uses the single gradient step to generate adversarial examples:

$$\begin{cases} x' = x + \epsilon \cdot \text{sign}(\nabla_x \mathcal{L}(x, y)) & \text{for untargeted} \\ x' = x - \epsilon \cdot \text{sign}(\nabla_x \mathcal{L}(x, t)) & \text{for targeted} \end{cases}, \quad (6)$$

where \mathcal{L} is the loss function. PGD is a multi-step method which create adversarial examples by iterative:

$$\begin{cases} x^{k+1} = \text{clip}(x^k + \alpha \cdot \text{sign}(\nabla_x \mathcal{L}(x^k, y))) & \text{for untargeted} \\ x^{k+1} = \text{clip}(x^k - \alpha \cdot \text{sign}(\nabla_x \mathcal{L}(x^k, t))) & \text{for targeted} \end{cases}, \quad (7)$$

where **clip** is the clip function, α is the step size of gradient, $x^0 = x$, $x' = x^K$ and K is the number of iterations. Also, some works [11, 31] use GANs to generate adversarial examples.

Adversarial training is a good and simple method to avoid adversarial examples, which improves the robustness of the neural networks by:

$$\min_{\theta} \mathbb{E}_{x, y \sim D} [\max_{\|\delta\|_p \leq \epsilon} \mathcal{L}_{\theta}(x + \delta, y)], \quad (8)$$

where $x, y \sim D$ is sampled from the joint distribution of data (image, label), θ is the parameter of the model. This min-max problem is similar to the GANs, the main difference is the independent variable of the maximization problem is image sample x in adversarial training, not parameters of the discriminator.

2.4. The Adversarial Robustness with GANs Training

Recently, some works begin to analyze the relationship between GANs training and adversarial robustness. Rob-

GAN [19] is the first work to introduce adversarial training in GANs training, which added the adversarial training for the classifier in cGANs. This method does not directly analyze that the discriminator of GANs is vulnerable to adversarial samples. Furthermore, Zhou et al [47] analyzed the non-robust characteristics of the discriminator for the first time. They proposed the consistent regularization between clean images and adversarial images in the training of GANs, which will let the discriminator not be fooled by adversarial examples. As we all know, adversarial training is a remarkable method to improve the adversarial robustness. Concurrent with our work, several methods [44, 18] independently proposed adversarial training for training of GANs. We urge the readers to check out their work for more details. Compared with concurrent works mentioned above, our paper analyzes the possibility of the generator to generate adversarial samples and the relationship between Direct Adversarial Training and adaptive Lipschitz minimum. Moreover, our work contains richer experiment results and better performance.

3. Condition of Adversarial Attacking by Generator

This section, we will prove the existence of the adversarial examples of discriminator during the GANs' training. Intuitively, the goals of adversarial training and generators' training are contradictory, while the goals of generator training and adversarial perturbation are the same. Both generator and adversarial perturbation hope that the generated distribution is closer to the true distribution under the metric of the discriminator.

Lemma 1. *Assuming δ is adversarial perturbation, ϕ^t and ϕ^{t+1} are the parameters for the t -th and $(t+1)$ -th update of the generator. Then the generator may generate adversarial examples of the discriminator*

The proof of the **Lemma 1** is shown in **subsection A.1 of the Appendix**. From **Lemma 1**, we can see that adversarial examples can be generated by generator, which confirms the validity of our previous assumptions.

4. Proposed Approach

Unlike previous adversarial training for classifiers, the proposed DAT method targeted at discriminator, which is a distribution metric function. The adversarial examples on the discriminator are defined as Eq (1), the unintentional attack for discriminator can be seen as a targeted attack, which minimizes the distance (under the discriminator) between the adversarial examples of the generated images and the real images, the same is true for adversarial examples of the real images.

In the following contents, we firstly introduce an adversarial perturbation strategy according to various distribution metrics, based on which the DAT method is proposed. Moreover, we also analyze the correlation between the proposed method and gradient penalty.

Algorithm 1 Direct Adversarial Training

Input: The batch size m , the real image distribution $P_r(x)$, the random noise $z \sim N(0, 1)$, the maximum number of training steps K , the number of steps to apply to the discriminator N , the loss function g_1 and g_2 , the parameter λ_1 and λ_2 .

Output: a fine-tuned generator G and discriminator D

```

1: for  $k=1, 2, \dots, K$  do
2:   for  $n=1, 2, \dots, N$  do
3:     Draw  $m$  real samples  $x_r = \{x_r^{(1)}, x_r^{(2)}, \dots, x_r^{(m)}\}$  from the real data distribution  $p_r(x)$ .
4:     Draw  $m$  latent noise  $z = \{z^{(1)}, z^{(2)}, \dots, z^{(m)}\}$ .
5:      $x_f = \{x_f^{(1)}, x_f^{(2)}, \dots, x_f^{(m)}\} = G_\phi(\{z^{(1)}, z^{(2)}, \dots, z^{(m)}\})$ 
6:      $\{\delta_f^{(1)}, \delta_f^{(2)}, \dots, \delta_f^{(m)}\} = -\epsilon \nabla_{x_f^{(i)}} (\|g_1(D(x_f^{(i)})) - \bar{g}_1(D(x_r))\|)$ 
7:      $\{\delta_r^{(1)}, \delta_r^{(2)}, \dots, \delta_r^{(m)}\} = -\epsilon \nabla_{x_r^{(i)}} (\|g_2(D(x_r^{(i)})) - \bar{g}_2(D(x_f))\|)$ 
8:      $x_{f-adv}^{(1)}, x_{f-adv}^{(2)}, \dots, x_{f-adv}^{(m)} = (\{x_f^{(1)} + \delta_f^{(1)}, x_f^{(2)} + \delta_f^{(2)}, \dots, x_f^{(m)} + \delta_f^{(m)}\})$ 
9:      $x_{r-adv}^{(1)}, x_{r-adv}^{(2)}, \dots, x_{r-adv}^{(m)} = (\{x_r^{(1)} + \delta_r^{(1)}, x_r^{(2)} + \delta_r^{(2)}, \dots, x_r^{(m)} + \delta_r^{(m)}\})$ 
10:    Update the discriminator by ascending its stochastic gradient:
          
$$\nabla_\theta \left\{ \frac{1}{m} \sum_{i=1}^m [g_1(D_\theta(x_{r-adv}^{(i)})) + g_2(D_\theta(x_{f-adv}^{(i)}))] \right\}$$

11:   end for
12:   Draw  $m$  latent noise  $\{z^{(1)}, z^{(2)}, \dots, z^{(m)}\}$ .
13:   Update the generator by descending its stochastic gradient:
          
$$\nabla_\phi \frac{-1}{m} \sum_{i=1}^m [g_1(D_\theta(x_r^{(i)})) + g_2(D_\theta(G_\phi(z^{(i)})))]$$

14: end for
15: return

```

4.1. Adversarial Perturbation of the Discriminator

Most of the adversarial training is about classifiers, the goal of the classifier is fixed. For untargeted attacks, the direction of adversarial perturbation is the solution of $\max \mathcal{L}(x, y)$; and for targeted attacks, the direction of adversarial perturbation is the solution of $\min \mathcal{L}(x, t)$, where \mathcal{L} is the loss function of the classifiers. But for discriminator, the goal of the output is dynamic, such as vanilla GAN, the outputs of the real images and fake images are both 0.5 for the optimal discriminator, but which is not true at the beginning of training. So the target of the output changes dynamically with training. Based on this, we propose a new adversarial perturbation for discriminator. Defining the optimization problem:

$$\begin{aligned} \delta(x_r) &= \arg \min \left| g_1(D_\theta(x_r + \delta(x_r))) - \overline{g_1(D_\theta(x_f))} \right|, \\ \delta(x_f) &= \arg \min \left| g_2(D_\theta(x_f + \delta(x_f))) - \overline{g_2(D_\theta(x_r))} \right|, \end{aligned} \quad (9)$$

where x_r and x_f are real image and generated image, respectively. $\delta(x_r)$ and $\delta(x_f)$ are adversarial perturbation of the real image x_r and generated image x_f , respectively. $\overline{g_1(D_\theta(x_r))}$ and $\overline{g_2(D_\theta(x_f))}$ are the average value of current discriminator output of the real images and generated images with a batch, respectively. For above optimization problem in Eq

(9). We use the one-step PGD attack to achieve it:

$$\begin{aligned} \delta(x_r) &= -\epsilon \nabla_{x_r} \left(\left| g_1(D(x_r)) - \overline{g_1(D(x_f))} \right| \right), \\ \delta(x_f) &= -\epsilon \nabla_{x_f} \left(\left| g_2(D(x_f)) - \overline{g_2(D(x_r))} \right| \right), \end{aligned} \quad (10)$$

where the goal of the adversarial perturbation changes with the training of the discriminator.

4.2. Direct Adversarial Training

Motivated by adversarial examples lead to unstable training of GANs, we propose an adversarial training DAT for GANs in Fig.2. According to the loss function of GANs in Eq (2), the loss of GANs with DAT can be written as:

$$\begin{aligned} \min_\phi \max_\theta f'(\phi, \theta) &= f_a(\phi, \theta) = \\ &\mathbb{E}_{x \sim p_r} [g_1(D_\theta(x + \delta(x_r)))] + \mathbb{E}_{z \sim p_z} [g_2(D_\theta(G_\phi(z) + \delta(x_f)))] \end{aligned} \quad (11)$$

According to the above formula, the complete algorithm is demonstrated in **Algorithm 1**.

4.3. Direct Adversarial Training and Lipschitz Continuous

In this part, we analyze the relationship between DAT and gradient penalty. The result demonstrates that our method

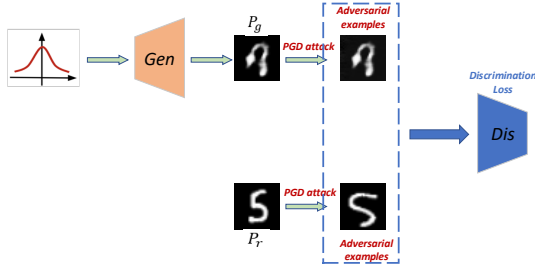


Figure 2: Illustration of the proposed method. This is similar to the GANs training. The difference is that we add the one-step PGD attack for real and generated images, we hope that the discriminator not only can identify real or fake, but also be robust to adversarial examples

can adjust the Lipschitz constant adaptively. The instability of GANs training is mainly caused by the discriminator, and our adversarial training is only for the discriminator, so we do not consider the generator at present. For adversarial perturbation of real images $\delta(x_r) = -\epsilon$.

$\nabla_{x_r} (|g_1(D(x_r)) - \overline{g_1(D(x_r))}|)$, the loss function of the discriminator can be written as:

$$\begin{aligned} & \max_{\theta} \mathbb{E}_{x \sim p_r} \left[g_1(D_{\theta}(x + \delta(x))) \right] \\ & \approx \max_{\theta} \mathbb{E}_{x \sim p_r} \left[g_1(D_{\theta}(x)) + \nabla_x g_1(D_{\theta}(x)) \cdot \delta(x) \right]. \end{aligned} \quad (12)$$

For loss function of the Eq (12):

$$\begin{aligned} & g_1(D_{\theta}(x_r)) + \nabla_{x_r} g_1(D_{\theta}(x_r)) \cdot \delta(x_r) \\ & = g_1(D_{\theta}(x_r)) - \epsilon \nabla_{x_r} g_1(D_{\theta}(x_r)) \\ & \quad \cdot \nabla_{x_r} \left| g_1(D_{\theta}(x_r)) - \overline{g_1(D_{\theta}(x_r))} \right| \\ & = g_1(D_{\theta}(x_r)) - \epsilon g_1' \nabla_{x_r} D_{\theta}(x_r) \\ & \quad \cdot \nabla_{x_r} \left| g_1(D_{\theta}(x_r)) - \overline{g_1(D_{\theta}(x_r))} \right|. \end{aligned} \quad (13)$$

Because x_f is sampled from fake images, which is independent of x_r , when $g_1(D_{\theta}(x_r)) - \overline{g_1(D_{\theta}(x_r))} \geq 0$, which is true in most cases, the Eq (13) is $g_1(D_{\theta}(x_r)) - \epsilon g_1'^2 \nabla_{x_r}^2 D_{\theta}(x_r)$. In this case, $\max g_1(D_{\theta}(x_r)) - \epsilon g_1'^2 \nabla_{x_r}^2 D_{\theta}(x_r)$ is equivalent to adding minimum gradient to loss, which can be seen as 0-GP. 0-GP can be used to limit the Lipschitz constant and stabilize the training of GANs. Also when $g_1(D_{\theta}(x_r)) - \overline{g_1(D_{\theta}(x_r))} < 0$, which means that the discriminator is trained incorrectly, the Eq (13) is $g_1(D_{\theta}(x_r)) + \epsilon g_1'^2 \nabla_{x_r}^2 D_{\theta}(x_r)$. In this case, $\max g_1(D_{\theta}(x_r)) + \epsilon g_1'^2 \nabla_{x_r}^2 D_{\theta}(x_r)$ means that we hope the discriminator will have a large change for perturbation, so as to jump out of the situation of wrong discrimination.

For adversarial perturbation of generated images $\delta(x_f) = -\epsilon \nabla_{x_f} (|g_2(D(x_f)) - \overline{g_2(D(x_f))}|)$, where $x_f = G_{\phi}(z)$. Up-

date of the discriminator can be written as:

$$\begin{aligned} & \max_{\theta} \mathbb{E}_{x \sim p_f} \left[g_2(D_{\theta}(x + \delta(x))) \right] \\ & \approx \max_{\theta} \mathbb{E}_{x \sim p_f} \left[g_2(D_{\theta}(x)) + \nabla_x g_2(D_{\theta}(x)) \cdot \delta(x) \right]. \end{aligned} \quad (14)$$

We can get the loss function similar to the real images:

$$\begin{aligned} & g_2(D_{\theta}(x_f)) - \epsilon g_2' \nabla_{x_f} D_{\theta}(x_f) \\ & \quad \cdot \nabla_{x_f} \left| g_2(D_{\theta}(x_f)) - \overline{g_2(D_{\theta}(x_f))} \right|. \end{aligned} \quad (15)$$

When $g_2(D_{\theta}(x_f)) \geq \overline{g_2(D_{\theta}(x_f))}$, the Eq (15) is $g_2(D_{\theta}(x_f)) - \epsilon g_2'^2 \nabla_{x_f}^2 D_{\theta}(x_f)$. For generated images x_f , usually, $g_2(D_{\theta}(x_f))$ is greater than $g_2(D_{\theta}(x_r))$, in this case the adversarial training is equivalent to 0-GP; and $g_2(D_{\theta}(x_f)) < \overline{g_2(D_{\theta}(x_f))}$ indicates that the discriminator has an error and may get the local saddle point, so we maximize the gradient of the discriminator $\nabla_{x_f}^2 D_{\theta}(x_f)$, which can make the discriminator jump out of the error point as soon as possible.

From the above analyses, it can be seen that our proposed DAT can adaptively minimize the Lipschitz continuity, which is equivalent to 0-GP when the discriminator performance is better, and relax the limit on the Lipschitz constant when the discriminator performance is poor.

5. Experiments

This section, we will introduce the impact of the DAT on DCGAN, WGAN, Spectral Normalization GAN (SNGAN) [23], Self-supervised GAN (SSGAN) [4] and Information Maximum GAN (InfoMAXGAN) [16]. The results show the effectiveness of our method. Furthermore, according to subsection 4.3, the proposed DAT can adaptively minimize the Lipschitz continuity. So we compare our method with other regularization and adversarial training methods, such as Gradient Penalty (GP) [9], Lipschitz Penalty (LP) [27], Minimum Gradient (0-GP) [48, 22, 37], Robust Regularization (AR and RFM) [47] and Adversarial Symmetric GAN (ASGAN) [18], in different loss functions. We set $\epsilon = 1$ in Eq 10 for all experiments.

5.1. Experiments on DCGAN

In this subsection, we use DCGAN to do experiments on two datasets to show the advance of our method. First, we evaluate our method on a 2D synthetic dataset, which is a mixture of nine Gaussians. The variance of the Gaussian distribution is 0.1, and the covariance is 0. We use a four layers of fully-connected MLP with 64 hidden units per layer to model the generator and discriminator. The Fig.3 illustrates the qualitative results of different iterations. The first line is visualization results on a **balanced** mixture of nine Gaussians. DAT can speed up the generation. When iterating 2k times, the generated distribution with adversarial training is closer to the true distribution. Even after training 10k times, the GANs without adversarial training can not fit the real distribution well. Also, we evaluate the method on an **imbalanced** mixture of nine Gaussians in second line. The results

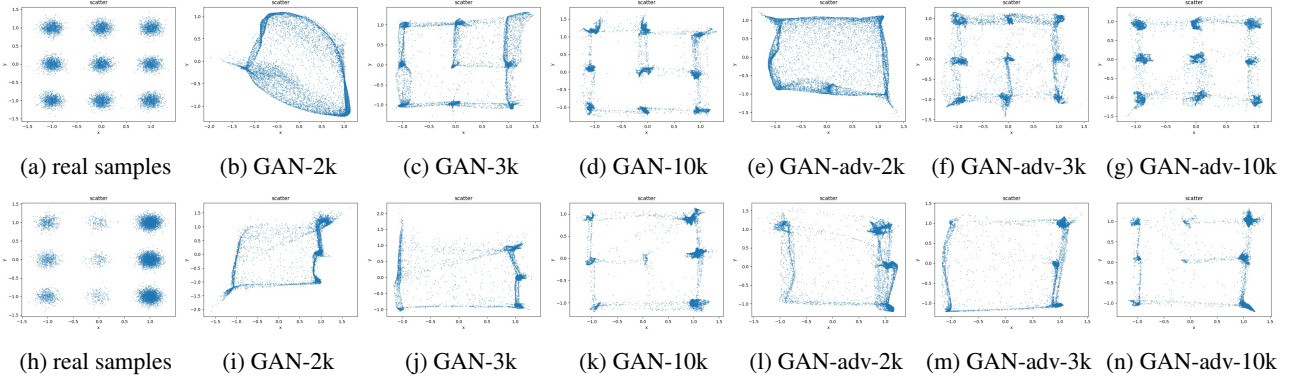


Figure 3: Qualitative results of nine 2D-Gaussian synthetic data. The first line is a **balanced** Gaussian mixture distribution, and the second line is an **imbalanced** Gaussian mixture distribution. **First line:** (a): the real samples from a mixture of nine Gaussians. Where variance is 0.1 and means are $\{-1, 0, 1\}$; (b), (c) and (d): the results of iterating 2k times, 3k times, and 10k times in DCGAN; (e), (f) and (g): the results of iterating 2k times, 3k times, and 10k times in DCGAN with DAT. **Second line:** (h): the real samples from an imbalanced mixture of nine Gaussians. The probability of mixing Gaussian from left to right is 0.15, 0.05, 0.8. The other parts are the same as the first line

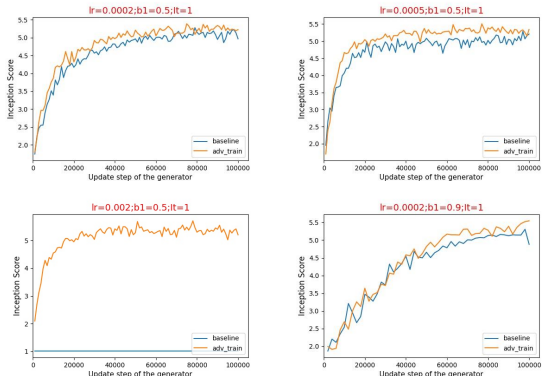


Figure 4: The results of the DCGAN with different parameters in CIFAR-10. Where 'lr' is learning rate, 'b1' is the parameter of the Adam optimizer, and 'It' is the ratio of the update times of the discriminator to the generator.

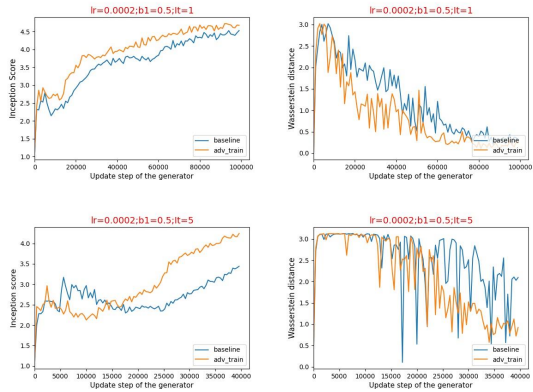


Figure 5: The results of the WGAN with different parameters in CIFAR-10. Where 'it' is the ratio of the update times of the discriminator to the generator.

illustrate that standard DCGAN will lose some small probability distribution, resulting in mode collapse, and this phenomenon will be significantly improved after DAT is added.

At the last, we use DCGAN¹ to do a comparative experiments on CIFAR-10 dataset [14], results are shown in Fig.4. From the results, under different parameters, the methods of direct adversarial training we proposed can improve the quality of the generated images. Especially when $lr=0.002$, $b1=0.5$, the standard DCGAN can not be trained due to the gradient vanishing. This shows that our direct adversarial training reduces the sensitivity to hyperparameters in the training of GANs and improves the stability of models.

5.2. Experiments on WGAN

This part, we use WGAN¹ to do a comparative experiments on CIFAR-10, the results are shown in Fig 5. From the results, the methods we proposed can achieve better performance. For Inception Score (IS), direct adversarial training can significantly improve the quality of generation. Especially when $it=5$, the training process falls into the local optimum in standard WGAN, which leads to a long-term decline in IS, and the time of the decline process is significantly shortened after using direct adversarial training, thereby reducing the difficulty of training. For Wasserstein distance, standard WGAN has obvious mutations in the training process. This mutation can be considered as the result of adversarial examples. When using adversarial training, the Wasserstein distance is smaller and more stable.

¹ This part, we do confirmatory experiments using simple architecture to implement DCGAN and WGAN. The dimension of the latent vector is set to 100. Generator and discriminator are all implemented by 4 convolution layers and BN layers. At the last, we use Adam optimizer.

Table 1
Training parameters on SOTA methods

Dataset	Resolution	Batch Size	Learning Rate	β_1	β_2	Decay Policy	n_{dis}	n_{iter}
CIFAR-10	32 × 32	64	2e-4	0.0	0.9	Linear	5	100K
CIFAR-100	32 × 32	64	2e-4	0.0	0.9	Linear	5	100K
STL-10	48 × 48	64	2e-4	0.0	0.9	Linear	5	100K
Tiny-ImageNet	64 × 64	64	2e-4	0.0	0.9	None	5	100K
LSUN-Bedroom	64 × 64	64	2e-4	0.0	0.9	Linear	5	100K

5.3. Evaluation on SOTA methods in different datasets

This subsection, we use DAT on some SOTA methods, such as SAGAN, SSGAN and InfoMAXGAN. The architectures used for all models are equivalent to SNGAN. They can be available on Github². We evaluate our method on five different datasets at multiple resolutions: CIFAR-10 (32×32) [14], CIFAR-100 (32 × 32) [14], STL-10 (48×48) [5], Tiny-ImageNet (64×64) [38], LSUN-Bedroom (64 × 64) [42]. See the Appendix A.2. for more detailed descriptions. All training parameters are selected the best results on baseline networks. The details can be found in Table 1, where the Adam parameters are Learning Rate (LR=2e-4), $\beta_1=0$ and $\beta_2=0.9$; n_{dis} is number of discriminator steps per generator step; n_{iter} is the trained times of the generator. Also, we use three metrics to evaluate the generated images quality: Fréchet Inception Distance (FID) [10], Kernel Inception Distance (KID) [2], and Inception Score (IS) [30]. In general, FID and KID measure the diversity between real and generated images, and IS only uses generated images to measure the quality. So we use train and test datasets to calculate FID and KID respectively. The results are illustrated on Table 2.

As seen in Table 2, DAT improves FID, KID, and IS consistently and significantly across many datasets with three popular models. This suggests our approach is versatile and can generalize across multiple data domains. In particular, the use of DAT greatly improved the FID of SSGAN in STL-10. Due to the large difference between the LSUN-Bedroom distribution and the ImageNet distribution, IS do not seem meaningful for it. So we do not show IS on LSUN-Bedroom dataset. Of course, there are some datasets where SSGAN with DAT has the best performance, and in some datasets, InfoMaxGAN with DAT has the best performance. Furthermore, there has a gap between Train FID and Test FID, as [46, 45] said, GAN also exists overfitting. This may be the direction of our future work.

Furthermore, we also provide image samples randomly generated for all datasets in Appendix A.3.

5.4. The FID Results on CIFAR-10 Dataset with Other Regularization Method

From Subsection 4.3, the DAT can be considered as an adaptive gradient minimum (0-GP) method. To demonstrate the advancements of our approach, we compare it with other

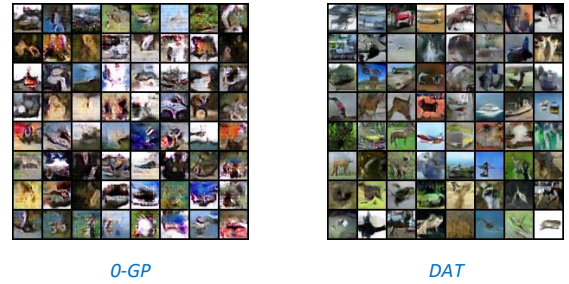


Figure 6: The results of the 0-GP and DAT with WGAN loss in CIFAR-10 dataset.

regularization methods, such as GP, LP, 0-GP, AR, RFM and ASGAN, on the CIFAR-10 dataset. To make the conclusion more general, we conduct comparative experiments on three losses of GANs (GAN [7], LSGAN [21], WGAN [1]). The baseline architecture and code are used to implement AR and RFM, which can be available on Github³. From which, the dimensions of the latent vector is 128, the batch size is 64, and the Adam optimizer is set to $lr = 0.0001$, $\beta_1 = 0.5$, $\beta_2 = 0.999$.

We have implemented LP, 0-GP, ASGAN and our method DAT and DATT based on the baseline. LP is a relaxation constraint of GP, and it limits the gradient of the discriminator to k ($k \leq 1$). 0-GP minimizes the gradient of the discriminator, which is similar to the DAT with adaptive gradient minimization. ASGAN is another method using adversarial training for discriminator. However, like using adversarial training in classification tasks, the adversarial examples in ASGAN are generated by $\hat{x} = x - \epsilon \operatorname{sign} \nabla_x (V_m(\theta, \phi, x, z))$, which is similar to the untargeted FGSM in Eq 6. $V_m(\theta, \phi, x, z)$ is the loss function of the discriminator. Here, we use the best-performing hyperparameter in [18], to be more specific, using FGSM on both real and fake samples and the key hyperparameter $\epsilon = \frac{1}{255}$. The FID results are shown in Table 3, where DAT represents training the GANs as shown in Algorithm 1, while DATT represents training the network with adversarial samples and normal samples together. The results confirm the advancements of our method. Specifically, we compare the generation results of 0-GP and DAT under the WGAN Loss, as shown in Fig.6. We find that the generation results on 0-GP with WGAN loss are very poor, which

²<https://github.com/kwotsin/mimicry>

³<https://github.com;bradyz/robust-discriminator-pytorch>

Table 2

FID, KID, and IS scores of SOTA models across different datasets. FID and KID: lower is better. IS: higher is better.

Metric	Dataset	Evaluation set	Models					
			SNGAN	SNGAN-DAT	SSGAN	SSGAN-DAT	InfoMaxGAN	InfoMaxGAN-DAT
FID	LSUN-Bedroom	Train	27.26	24.10	23.54	20.43	35.69	34.21
		Test	86.10	83.50	85.10	82.20	87.14	86.17
	Tiny-ImageNet	Train	47.14	43.40	40.83	38.98	41.81	38.83
		Test	52.29	48.72	45.79	44.63	47.26	43.97
	STL-10	Train	42.62	41.05	39.84	35.64	42.39	40.77
		Test	62.03	60.41	56.56	52.71	61.93	59.07
	CIFAR-100	Train	23.70	21.09	22.43	19.86	21.36	20.46
		Test	28.48	26.49	27.61	24.67	26.36	25.28
	CIFAR-10	Train	20.05	17.93	16.75	15.34	17.71	17.69
		Test	24.19	22.46	21.23	19.45	22.03	21.88
KID	LSUN-Bedroom	Train	0.0313	0.0286	0.0267	0.0246	0.0373	0.0369
		Test	0.0324	0.0296	0.0298	0.0275	0.0388	0.0375
	Tiny-ImageNet	Train	0.0411	0.0391	0.0355	0.0337	0.0371	0.0323
		Test	0.0415	0.0393	0.0371	0.0341	0.0372	0.0332
	STL-10	Train	0.0391	0.0380	0.0388	0.0336	0.0418	0.0384
		Test	0.0445	0.0428	0.0403	0.0352	0.0443	0.0404
	CIFAR-100	Train	0.0158	0.0160	0.0155	0.0147	0.0152	0.0140
		Test	0.0164	0.0161	0.0160	0.0148	0.0153	0.0142
	CIFAR-10	Train	0.0149	0.0133	0.0125	0.0116	0.0134	0.0128
		Test	0.0150	0.0142	0.0128	0.0118	0.0139	0.0141
IS	LSUN-Bedroom	None	-	-	-	-	-	-
	Tiny-ImageNet	None	8.17	8.44	8.63	8.95	8.80	9.18
	STL-10	None	8.34	8.45	8.59	8.72	8.28	8.57
	CIFAR-100	None	7.66	7.82	7.74	8.09	8.02	8.06
	CIFAR-10	None	7.84	7.97	8.13	8.25	8.01	8.07

Table 3

FID scores on CIFAR-10 for various GAN losses and regularization.

loss	regularization								
	None	GP[9]	LP[27]	0-GP	AR[47]	RFM[47]	ASGAN[18]	DAT(ours)	DATT(DAT+T)
GAN[7]	30.20	27.80	27.25	29.76	29.37	27.89	27.24	26.98	26.77
LSGAN[21]	25.20	24.40	25.38	28.67	26.49	26.05	26.46	24.38	24.35
WGAN[1]	29.43	26.03	26.90	43.06	27.26	26.83	25.98	25.67	25.66

may be caused by the strong limit of minimizing the gradient penalty. DAT will adaptively minimize the gradient, which relieves the above limitation to improve the quality of the generation.

6. Conclusions

Motivated by adversarial examples may affect the stable training of the GANs, in this paper, we use the direct adversarial training for GANs. Since the discriminator is a distributed metric function, based on this, we propose a new adversarial perturbation for the discriminator. Of course, we prove the existence of adversarial examples of the discriminator. At last, we also prove that this kind of adversarial training can adaptively adjust the Lipschitz continuous,

which can improve stability of the training and the quality of generated images.

Acknowledgment

The work is partially supported by the National Natural Science Foundation of China under grand No.U19B2044, No.61836011.

References

- [1] Arjovsky, M., Chintala, S., Bottou, L., 2017. Wasserstein gan. arXiv preprint arXiv:1701.07875 .
- [2] Bińkowski, M., Sutherland, D.J., Arbel, M., Gretton, A., 2018. Demystifying mmd gans. arXiv preprint arXiv:1801.01401 .

[3] Bonnotte, N., 2013. From knothe's rearrangement to brenier's optimal transport map. *SIAM Journal on Mathematical Analysis* 45, 64–87.

[4] Chen, T., Zhai, X., Ritter, M., Lucic, M., Houlsby, N., 2019. Self-supervised gans via auxiliary rotation loss, in: *Proceedings of the IEEE Conference on Computer Vision and Pattern Recognition*, pp. 12154–12163.

[5] Coates, A., Ng, A., Lee, H., 2011. An analysis of single-layer networks in unsupervised feature learning, in: *Proceedings of the International Conference on Artificial Intelligence and Statistics*, pp. 215–223.

[6] Couellan, N., 2019. The coupling effect of lipschitz regularization in deep neural networks. *arXiv preprint arXiv:1904.06253* .

[7] Goodfellow, I., Pouget-Abadie, J., Mirza, M., Xu, B., Warde-Farley, D., Ozair, S., Courville, A., Bengio, Y., 2014a. Generative adversarial nets, in: *Advances in neural information processing systems*, pp. 2672–2680.

[8] Goodfellow, I.J., Shlens, J., Szegedy, C., 2014b. Explaining and harnessing adversarial examples. *arXiv preprint arXiv:1412.6572* .

[9] Gulrajani, I., Ahmed, F., Arjovsky, M., Dumoulin, V., Courville, A.C., 2017. Improved training of wasserstein gans, in: *Advances in Neural Information Processing Systems*, pp. 5767–5777.

[10] Heusel, M., Ramsauer, H., Unterthiner, T., Nessler, B., Hochreiter, S., 2017. Gans trained by a two time-scale update rule converge to a local nash equilibrium. *Advances in Neural Information Processing Systems* 30, 6626–6637.

[11] Hu, W., Tan, Y., 2017. Generating adversarial malware examples for black-box attacks based on gan. *arXiv preprint arXiv:1702.05983* .

[12] Kantorovich, L.V., 2006. On a problem of monge. *J. Math. Sci.(NY)* 133, 1383.

[13] Kodali, N., Abernethy, J., Hays, J., Kira, Z., 2017. On convergence and stability of gans. *arXiv preprint arXiv:1705.07215* .

[14] Krizhevsky, A., Hinton, G., et al., 2009. Learning multiple layers of features from tiny images .

[15] Kurakin, A., Goodfellow, I., Bengio, S., 2016. Adversarial machine learning at scale. *arXiv preprint arXiv:1611.01236* .

[16] Lee, K.S., Tran, N.T., Cheung, N.M., 2020. Infomax-gan: Improved adversarial image generation via information maximization and contrastive learning. *arXiv preprint arXiv:2007.04589* .

[17] Li, Z., Tao, R., Li, B., 2020. Regularization and normalization for generative adversarial networks: A review. *arXiv preprint arXiv:2008.08930* .

[18] Liu, F., Xu, M., Li, G., Pei, J., Shi, L., Zhao, R., 2020. Adversarial symmetric gans: Bridging adversarial samples and adversarial networks. *Neural Networks* .

[19] Liu, X., Hsieh, C.J., 2019. Rob-gan: Generator, discriminator, and adversarial attacker, in: *Proceedings of the IEEE Conference on Computer Vision and Pattern Recognition*, pp. 11234–11243.

[20] Madry, A., Makelov, A., Schmidt, L., Tsipras, D., Vladu, A., 2017. Towards deep learning models resistant to adversarial attacks. *arXiv preprint arXiv:1706.06083* .

[21] Mao, X., Li, Q., Xie, H., Lau, R.Y., Wang, Z., Paul Smolley, S., 2017. Least squares generative adversarial networks, in: *Proceedings of the IEEE International Conference on Computer Vision*, pp. 2794–2802.

[22] Mescheder, L., Geiger, A., Nowozin, S., 2018. Which training methods for gans do actually converge? *arXiv preprint arXiv:1801.04406* .

[23] Miyato, T., Kataoka, T., Koyama, M., Yoshida, Y., 2018a. Spectral normalization for generative adversarial networks. *arXiv preprint arXiv:1802.05957* .

[24] Miyato, T., Maeda, S.i., Koyama, M., Ishii, S., 2018b. Virtual adversarial training: a regularization method for supervised and semi-supervised learning. *IEEE Transactions on Pattern Analysis and Machine Intelligence* 41, 1979–1993.

[25] Nowozin, S., Cseke, B., Tomioka, R., 2016. f-gan: Training generative neural samplers using variational divergence minimization, in: *Advances in Neural Information Processing Systems*, pp. 271–279.

[26] Oberman, A.M., Calder, J., 2018. Lipschitz regularized deep neural networks converge and generalize. *arXiv preprint arXiv:1808.09540* .

[27] Petzka, H., Fischer, A., Lukovnicov, D., 2017. On the regularization of wasserstein gans. *arXiv preprint arXiv:1709.08894* .

[28] Qi, G.J., 2020. Loss-sensitive generative adversarial networks on lipschitz densities. *International Journal of Computer Vision* 128, 1118–1140.

[29] Radford, A., Metz, L., Chintala, S., 2015. Unsupervised representation learning with deep convolutional generative adversarial networks. *arXiv preprint arXiv:1511.06434* .

[30] Salimans, T., Goodfellow, I., Zaremba, W., Cheung, V., Radford, A., Chen, X., 2016. Improved techniques for training gans. *Advances in Neural Information Processing Systems* 29, 2234–2242.

[31] Samangouei, P., Kabkab, M., Chellappa, R., 2018. Defense-gan: Protecting classifiers against adversarial attacks using generative models. *arXiv preprint arXiv:1805.06605* .

[32] Shen, Y., Gu, J., Tang, X., Zhou, B., 2020. Interpreting the latent space of gans for semantic face editing, in: *Proceedings of the IEEE Conference on Computer Vision and Pattern Recognition*, pp. 9243–9252.

[33] Song, Y., Shu, R., Kushman, N., Ermon, S., 2018. Constructing unrestricted adversarial examples with generative models, in: *Advances in Neural Information Processing Systems*, pp. 8312–8323.

[34] Szegedy, C., Zaremba, W., Sutskever, I., Bruna, J., Erhan, D., Goodfellow, I., Fergus, R., 2013. Intriguing properties of neural networks. *arXiv preprint arXiv:1312.6199* .

[35] Tao, R., Li, Z., Tao, R., Li, B., 2019. Resattr-gan: Unpaired deep residual attributes learning for multi-domain face image translation. *IEEE Access* 7, 132594–132608.

[36] Terjék, D., 2019. Adversarial lipschitz regularization, in: *International Conference on Learning Representations*.

[37] Thanh-Tung, H., Tran, T., Venkatesh, S., 2019. Improving generalization and stability of generative adversarial networks. *arXiv preprint arXiv:1902.03984* .

[38] Wu, J., Zhang, Q., Xu, G., . Tiny ImageNet Challenge. Technical Report.

[39] Xiao, C., Li, B., Zhu, J.Y., He, W., Liu, M., Song, D., 2018. Generating adversarial examples with adversarial networks. *arXiv preprint arXiv:1801.02610* .

[40] Yeh, R.A., Chen, C., Yian Lim, T., Schwing, A.G., Hasegawa-Johnson, M., Do, M.N., 2017. Semantic image inpainting with deep generative models, in: *Proceedings of the IEEE Conference on Computer Vision and Pattern Recognition*, pp. 5485–5493.

[41] Yoshida, Y., Miyato, T., 2017. Spectral norm regularization for improving the generalizability of deep learning. *arXiv preprint arXiv:1705.10941* .

[42] Yu, F., Seff, A., Zhang, Y., Song, S., Funkhouser, T., Xiao, J., 2015. Lsun: Construction of a large-scale image dataset using deep learning with humans in the loop. *arXiv preprint arXiv:1506.03365* .

[43] Yu, J., Lin, Z., Yang, J., Shen, X., Lu, X., Huang, T.S., 2018. Generative image inpainting with contextual attention, in: *Proceedings of the IEEE Conference on Computer Vision and Pattern Recognition*, pp. 5505–5514.

[44] Zhang, S., Qian, Z., Huang, K., Xiao, J., He, Y., 2020. Robust generative adversarial network. *arXiv preprint arXiv:2004.13344* .

[45] Zhao, S., Liu, Z., Lin, J., Zhu, J.Y., Han, S., 2020a. Differentiable augmentation for data-efficient gan training. *Advances in Neural Information Processing Systems* 33.

[46] Zhao, Z., Zhang, Z., Chen, T., Singh, S., Zhang, H., 2020b. Image augmentations for gan training. *arXiv preprint arXiv:2006.02595* .

[47] Zhou, B., Krähenbühl, P., 2018. Don't let your discriminator be fooled, in: *International Conference on Learning Representations*.

[48] Zhou, Z., Liang, J., Song, Y., Yu, L., Wang, H., Zhang, W., Yu, Y., Zhang, Z., 2019a. Lipschitz generative adversarial nets. *arXiv preprint arXiv:1902.05687* .

[49] Zhou, Z., Shen, J., Song, Y., Zhang, W., Yu, Y., 2019b. Towards efficient and unbiased implementation of lipschitz continuity in gans. *arXiv preprint arXiv:1904.01184* .

A. Appendix

A.1. The Proof of the Lemma 1

Lemma 2. Assuming δ is adversarial perturbation, ϕ^t and ϕ^{t+1} are the parameters for the t -th and $(t+1)$ -th update of the generator. Then the generator may generate adversarial examples of the discriminator

Proof 1:

- Suppose that the loss function between the true distribution and the generated distribution measured by the discriminator is \mathcal{L} , the generator is single-layered which can be represented as $G_\phi(z) = f(\phi \cdot z)$. Having:

$$\begin{aligned} D_\theta(G(z; \phi^{t+1})) &= D_\theta(G(z; \phi^t + \Delta\phi)) \\ &= D_\theta(f(z \cdot (\phi^t + \Delta\phi))) \\ &= D_\theta(f(z \cdot \phi^t) + \nabla f \Delta\phi \cdot z) \\ &= D_\theta(G_\phi(z) + \nabla f \Delta\phi \cdot z) \end{aligned} \quad (16)$$

where $\Delta\phi = \phi^{t+1} - \phi^t$ is the updated value of the generator parameters, f is activation function. If using SGD, then $\Delta\phi = \frac{\partial \mathcal{L}}{\partial \phi}$. Also the adversarial perturbation $\delta = \frac{\partial \mathcal{L}}{\partial G_\phi(z)}$. For $\frac{\partial \mathcal{L}}{\partial \phi} = \frac{\partial \mathcal{L}}{\partial G_\phi(z)} \nabla f \cdot z$, having:

$$D_\theta(G(z; \phi^{t+1})) = D_\theta(G_\phi(z) + \delta \nabla^2 f \cdot z^2) \quad (17)$$

If $\nabla^2 f \cdot z^2 = 1$, then the generator will generate the adversarial examples of the discriminator.

- If the generator is two-layered, which can be represented as $G_\phi(z) = f_2(\phi_2 \cdot f_1(\phi_1 \cdot z))$. Having:

$$D_\theta(G(z; \phi^{t+1})) = D_\theta(G(z; \phi^t + \Delta\phi)) \quad (18)$$

$D_\theta(G(z; \phi_1^{t+1}))$ can be writed as:

$$\begin{aligned} D_\theta(G(z; \phi_1^{t+1})) &= D_\theta(G(z; \phi_1^t + \Delta\phi_1)) \\ &= D_\theta(f_2(\phi_2^t \cdot f_1(z \cdot (\phi_1^t + \Delta\phi_1)))) \\ &= D_\theta(G_\phi(z) + \nabla f_2 \nabla f_1 \Delta\phi_1 \cdot \phi_2^t \cdot z) \end{aligned} \quad (19)$$

Now, the adversarial perturbation $\delta = \frac{\partial \mathcal{L}}{\partial G_\phi(z)}$. For $\frac{\partial \mathcal{L}}{\partial \phi_1} = \frac{\partial \mathcal{L}}{\partial G_\phi(z)} \nabla f_2 \nabla f_1 \cdot \phi_2 \cdot z$, having:

$$D_\theta(G(z; \phi_1^{t+1})) = D_\theta(G_\phi(z) + \delta \nabla^2 f_2 \nabla^2 f_1 \cdot \phi_2^2 \cdot z^2) \quad (20)$$

Similarly, $D_\theta(G(z; \phi_2^{t+1}))$ can be writed as:

$$\begin{aligned} D_\theta(G(z; \phi_2^{t+1})) &= D_\theta(G(z; \phi_2^t + \Delta\phi_2)) \\ &= D_\theta(f_2((\phi_2^t + \Delta\phi_2) \cdot f_1(z \cdot \phi_1^t))) \\ &= D_\theta(G_\phi(z) + \nabla f_2 \Delta\phi_2 f_1(\phi_1^t \cdot z)) \end{aligned}$$

Now, the adversarial perturbation $\delta = \frac{\partial \mathcal{L}}{\partial G_\phi(z)}$. For $\frac{\partial \mathcal{L}}{\partial \phi_2} = \frac{\partial \mathcal{L}}{\partial G_\phi(z)} \nabla f_2 \cdot f_1(\phi_1 \cdot z)$, having:

$$D_\theta(G(z; \phi_2^{t+1})) = D_\theta(G_\phi(z) + \delta \nabla^2 f_2 \cdot f_1^2(\phi_1 \cdot z)) \quad (22)$$

If $\nabla^2 f_2 \nabla^2 f_1 \cdot \phi_2^2 \cdot z^2 = 1$ and $\nabla^2 f_2 \cdot f_1^2(\phi_1 \cdot z) = 1$, then the generator will generate the adversarial examples of the discriminator.

- Similarly, the multi-layered generator $G_\phi(z) = f_3(\phi_3 \cdot f_2(\phi_2 \cdot f_1(\phi_1 \cdot z)))$, which will also generate adversarial examples of the discriminator. The proof is similar to the previous two points.

□

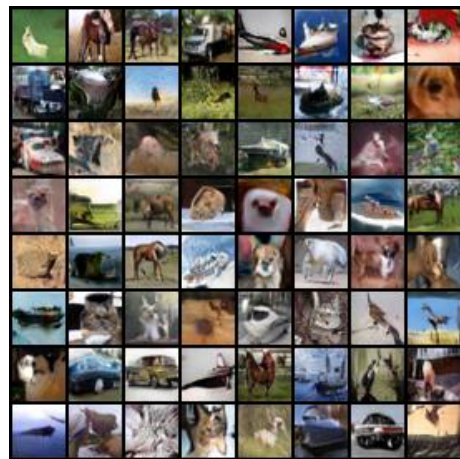
Lemma 1 aims to show that the generator may generate adversarial examples of the discriminator. The proof is not strict. We just explore the possibility of this phenomenon existing.

A.2. The Details of Datasets in Subsection 5.3.

We use IS, Train FID, Test FID, Train KID, and Test KID to demonstrate the advancements of DAT on five datasets in Subsection 5.3. Since FID and KID are calculated on different sets, this Subsection describes the set of datasets. CIFAR-10 and CIFAR-100 comprise 50K training images and 10K test images with a spatial resolution of 32×32 . Thus we train GAN models and compute Train FID on the training dataset with 50K images. Certainly, Test FID is calculated on the test dataset with 10K images. STL-10 is a similar dataset that contains 100K unlabeled images and 8K test images at 96×96 resolution. We resize them to 48×48 . Thus we train GAN models on the whole unlabeled dataset and compute Train FID on the unlabeled dataset with random 50000 images. Certainly, Test FID is calculated on the test dataset with 8000 images. Tiny ImageNet contains 200 image classes, a training dataset of 100K images and a test dataset of 10K images. All images are of size 64×64 . Similarly, we train GAN models on the whole training dataset and compute Train FID on the training dataset with 50K random images. Certainly, Test FID is calculated on the test dataset with 10K images. LSUN Bedroom has approximately 3M images. We took out 10K of them as a test set which is used to calculate the Test FID. Certainly, we compute Train FID on the training dataset with 50000 random images.

A.3. Generated Image Samples

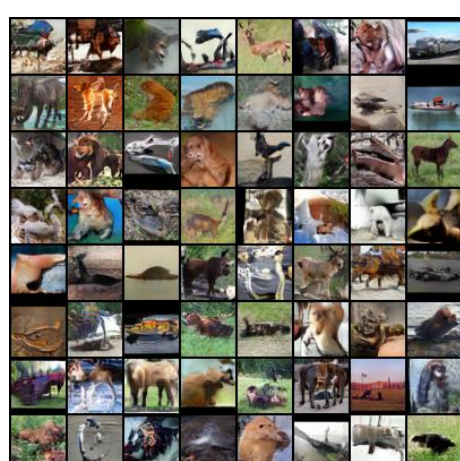
For qualitative comparisons, we present randomly sampled, non-cherry picked images generated by SSGAN and SSGAN-DAT for CIFAR-10, CIFAR-100, STL-10 and LSUN-Bedroom in Figures 7 and 8. We qualitatively observe that the images are more diverse and have higher quality after the use of DAT.



(a) CIFAR10

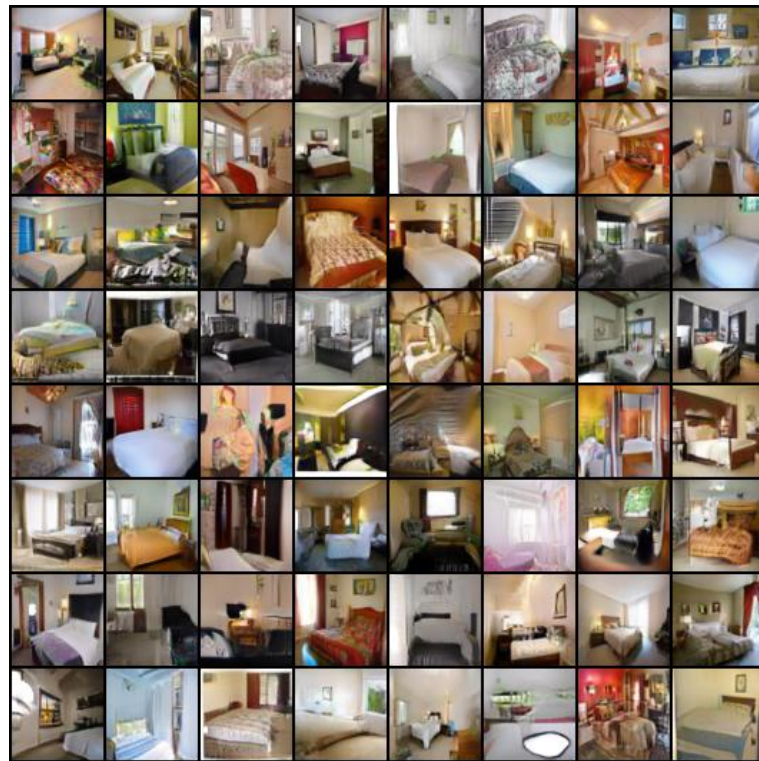


(b) CIFAR100

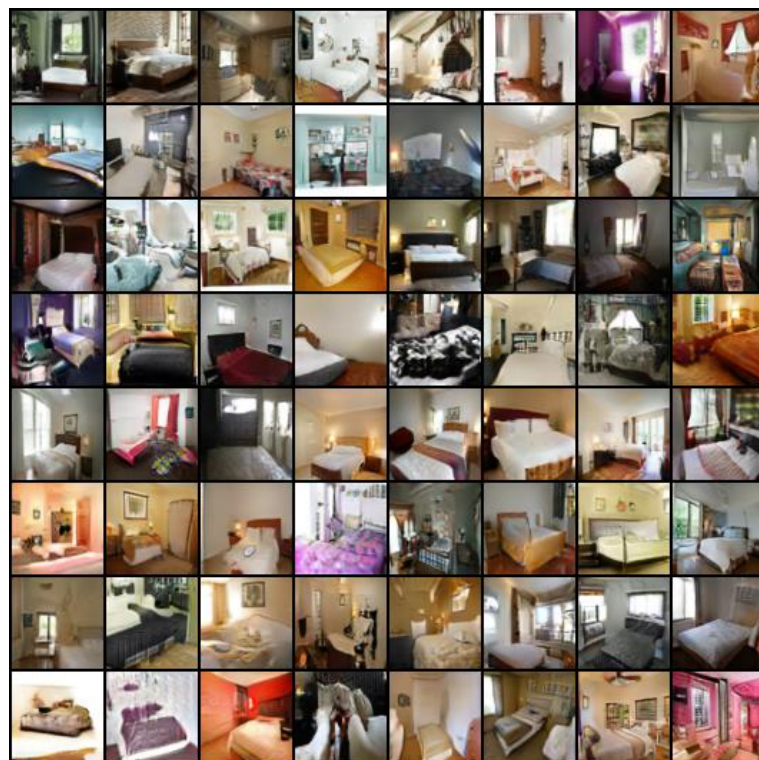


(c) STL10

Figure 7: Randomly sampled and non-cherry picked images for SSGAN (left) and SSGAN-DAT (right) for CIFAR-10, CIFAR-100, and STL-10 datasets.



(a) SSGAN



(b) SSGAN-DAT

Figure 8: Randomly sampled and non-cherry picked images for SSGAN (top) and SSGAN-DAT (bottom) for LSUN-Bedroom dataset.